

# **Pharmacological PARP-1 Inhibition Against Hypertensive Target Organ Damage in a Chronic Animal Model**

Ph.D. Thesis

**Author:** Krisztián Erős, MSc.

**Program Leader:** Prof. Kálmán Tóth, M.D., Sc.D.

**Project Leader:** Róbert Halmosi, M.D., Ph.D.



1<sup>st</sup> Department of Medicine  
University of Pécs, Medical School  
Hungary

2017

## **1. Introduction**

### **1.1. Hypertension and related complications**

Arterial hypertension represents a major cardiovascular epidemic condition, with a prevalence of more than 25% throughout the adult population, affecting nearly one billion individuals around the globe. It remains asymptomatic until later in its course, but as a long-term consequence of this condition, accumulating damage in specific organs emerges. Complex biochemical, hormonal and hemodynamic mechanisms form the basis of these alterations, referred as hypertensive target organ damage/TOD, however, the common ground is the excess generation of reactive oxygen species/ROS, which, in addition to modulating intracellular signaling routes, possesses direct damaging properties against biomolecules. In the vasculature, these species are formed by all cellular components such as endothelial cells, smooth muscle fibers, fibroblasts and activated immune cells.

While various kinds of ROS participate in physiological vascular functions, an imbalance in their production and elimination during pathological situations, defined as oxidative stress, leads to permanent functional and structural changes in the cardiovascular system and, also in the supplied tissues. The main enzymatic sources of excess ROS production are the NADPH oxidases, xanthine oxidase and the mitochondrial electron transfer chain/ETC. In the oxidatively stressed vasculature, the potent vasodilator nitrogen monoxide/NO quickly reacts with superoxide anion/ $O_2^-$  to form the highly reactive peroxynitrite/ $ONOO^-$ . This reaction, in the process of reducing NO bioavailability, additionally propagating endothelial nitrogen monoxide synthase/eNOS uncoupling, leading to the dysregulation of vascular tone. Also, this product potentially induces damage of lipoproteins by forming nitrotyrosine/NT adducts, altering their structure and function.  $ONOO^-$  is also a potent inducer of oxidative DNA modification, and in this manner, activates the nuclear enzyme poly(ADP-ribose)polymerase-1/PARP-1, a DNA damage sensor positioned centrally in the cellular stress response.

### **1.2. Processes in chronic hypertension-related cardiovascular remodeling, tissue damage and the spontaneously hypertensive rat model**

The spontaneously hypertensive rat/SHR strain was developed in the 1960's by Professor Kyuzo Aoki and colleagues, via the selective inbreeding of Wistar-Kyoto /WKY rats with consistently elevated blood pressure. Since then, it has become one of the most intensively

studied organisms in experimental cardiology with pathologies resembling human essential hypertension.

During chronic hypertension, as a resultant of hemodynamic factors, altered neurohumoral activity and an imbalance in vasodilator and constrictor forces, the vasculature displays adaptive changes that influence their diameter and vasomotor responses governed by the structural reorganization of the vascular wall. Various signaling routes mediate these processes of vascular remodeling, in which Ang II initiated ROS-dependent signaling, activation of the mitogen-activated protein kinase/MAPK system and inflammatory processes governed by nuclear factor kappa-light-chain-enhancer of activated B cells/NF- $\kappa$ B function possess dominant contribution.

Alterations of the central nervous system on the grounds of chronic hypertension are primarily mediated by the cerebrovascular changes and deteriorated blood-brain barrier/BBB function induced by inflammatory processes and oxidative damage. The progressive remodeling of the cerebral vasculature results in cerebral hypoperfusion. In this regard the hippocampus is particularly sensitive to ischemic insults and represents a predilection site for brain damage following disturbances in blood supply or dysfunction of the BBB. However, neurodegenerative processes of the hippocampus are studied mainly during acute ischemia/reperfusion damage, the SHR strain may represent a chronic animal model for the hypertension-related cerebral pathologies.

In regard to the heart, the hypertension related alterations are primarily the results of the hypertrophic response of the cardiac wall, aiding to maintain cardiac work and oxygen supply of tissues in the face of the altered peripheral resistance. Above a specific threshold, the progression of wall thickening induces pathological changes due to the improper oxygen supply and metabolic alterations of cardiomyocytes, resulting in structural remodeling accompanied by fibrotic tissue accumulation and cell death. Insufficient bioenergetic adaptation and disturbances in the processes controlling mitochondrial quality, composed by fusion, fission and selective elimination (mitophagy) events, have all emerged as key factors in the transition to pathological remodeling of the continuously working, highly energy-demanding cardiac muscle.

### **1.3. Physiological functions of the nuclear PARP-1 enzyme and its role during stress**

PARP-1 functions as a DNA damage sensor and participates in the recruitment and function of the DNA repair machinery under low or mild genotoxic damage. Also, via its

interaction with various nuclear proteins like transcription factors and chromatin modifiers, it is capable of regulating wide-scale transcriptional programs in a chromatin-dependent manner. Interactions of stress related PARP-1 activity have been also demonstrated by crucial intracellular signaling routes, governing inflammatory processes via NF- $\kappa$ B co-activation, cellular stress adaptation and cell fate decisions. During prolonged or excessive genotoxic stress, PARP-1 becomes hyperactivated and diminishes the nuclear NAD<sup>+</sup> pool. In this fashion, its excess activation limits the functionality of other NAD<sup>+</sup> dependent nuclear enzymes, such as the Sirtuins, and also drives the cell towards a metabolic catastrophe by impaired glycolysis and excess adenosine triphosphate/ATP usage. Originally, this mechanism was considered as the main initiator of the caspase-independent regulated necrosis termed as parthanatos, as stated by the Berger's suicide model. During PARP-1 mediated necroptosis, the mitochondria may represent a key control point. In an oxidatively stressed cellular model, parthanatos was accompanied by gross mitochondrial depolarization, secondary O<sub>2</sub><sup>-</sup> production and elevated intracellular Ca<sup>++</sup> levels. Mitochondria also displayed the severely damaged ultrastructure of swollen organelles, which alterations could be prevented by PARP-1 deficiency or its pharmacological inhibition.

Traditionally, deleterious consequences of excess PARP-1 activation were studied in acute stress scenarios associated with oxidative DNA damage, such as ischemia-reperfusion or in models in which DNA damage was induced by alkylating agents or irradiation. Later, profound roles of PARP-1 in tissue damage were also demonstrated in chronic diseases characterized by the augmented levels of ROS, such as diabetes mellitus or hypertension.

## **2. Objectives / Specific Aims**

We aimed to observe signs of the elevated oxidative stress in various tissues of SHR animals and elucidate mechanisms of their contribution to chronic hypertension-induced TOD, with a special emphasis on the role of PARP-1 activation during these processes.

**Specific Aim I.** Evaluation of chronic hypertension-induced vascular remodeling in SHR animals at the level of carotid arteries, in light of long-term pharmacological inhibition of PARP-1.

Structural and functional remodeling of various vascular segments already described in SHR animals includes damages and dysfunction of the endothelial layer, changes in lumen

diameter and wall thickness with fibrotic tissue accumulation. In this specific aim, at the level of carotid arteries, we monitor these processes strongly related to an elevated level of oxidative stress present in the vasculature of this strain. In addition to initiating oxidative DNA damage related cell death events, intracellular signaling interactions of PARP-1 activity in the stressed vasculature may propagate its phenotypical changes. In this way, level and subcellular distribution of the main regulators of cell death, inflammatory processes and MAPK activity are assessed.

**Specific Aim II. Observation of chronic hypertension related alterations of the dorsal hippocampus in the SHR strain, focusing on the level of oxidative stress and cell death events.**

One of the most deleterious consequences of hypertension-induced vascular remodeling is the inadequate perfusion of the supplied tissues. As the brain is a highly energy-demanding organ with low ischemic tolerance, attenuating the vascular alterations during chronic hypertension is presumably beneficial in various forms of dementias. Furthermore, the protection of neuronal tissue is highly dependent on the structure of BBB, the integrity of which is deteriorated in chronic hypertension due to inflammatory processes and endothelial damage. In this aim, in conjunction with pharmacological PARP-1 activity modulation, we specifically focus on markers of oxidative stress related tissue damage and cell loss in the dorsal hippocampus, as a cerebral model area for hypertensive target organ damage in the SHR strain.

**Specific Aim III. To elucidate evidences of mitochondrial protection achieved by PARP-1 inhibition in the myocardium.**

During persistent hypertension, cardiac muscle adapts to the increased workload by hypertrophy. The metabolic adaptation capabilities of cardiac mitochondria are fundamental to maintain proper cardiac function during this compensatory phase. Disturbed processes of mitochondrial quality control and a metabolic insufficiency propagate the progression of cardiac dysfunction with myocyte loss, leading to eventual heart failure. The mitochondria are highly dynamic organelles, which reacts to a perturbative environment by a shift in the fusion-fission equilibrium. In this specific aim, we seek to make qualitative assessments on the ultrastructural level and to quantify the actual state of mitochondrial fusion-fission processes in the hypertrophied myocardium. Also, the effect of long-term L-2286 PARP-1 inhibitor

treatment on levels of DRP1 and OPA1 is assessed in whole cell preparations and subcellular fractions.

### 3. Materials and Methods

#### 3.1. Chemicals

The water soluble PARP-1 inhibitor 2-[(2-Piperidine-1-ylethyl)thio]quinazolin-4(3H)-one (L-2286) (Fig.1.) was a kind and generous gift of Professor Kalman Hideg and Professor Tamas Kalai, from the Department of Organic and Pharmacological Chemistry (Medical School, University of Pecs, Hungary). The compound was chosen from a group of experimental 4-quinazolinone derivatives, synthesized based on the crystal structure of the PARP-1 catalytic domain. The *in vitro* measurements demonstrated an IC<sub>50</sub> of 2.6 μM against isolated human PARP-1.

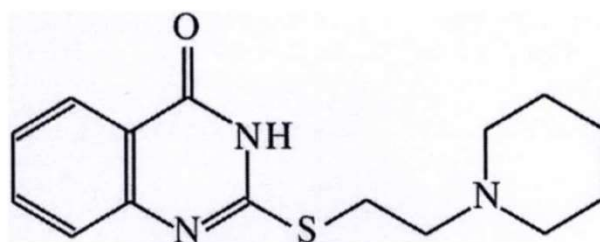


**Figure 1.: Chemical structure of L-2286 (2-[(2-Piperidine-1-ylethyl) thio] quinazolin-4 (3H)-one)**

#### 3.2. Animals

Male SHR animals aged at 10 weeks and serving in the role of normotensive controls, age-matched WKY rats were purchased from Charles River Laboratories (Budapest, Hungary). Animals were caged individually and maintained on a 12 h light/dark cycle at 24 °C. Following ultrasound examinations to exclude animals with carotid artery abnormalities, each strain was randomized into groups (n=15/group) receiving 5 mg/kg/day L-2286 treatment (WKY-L and SHR-L) or not (WKY-C and SHR-C) for 32 weeks.

### **3.3. Blood pressure measurement**

Non-invasive blood pressure measurements were carried out every four weeks from the beginning of the study using the tail-cuff method. A heating pad was applied to maintain normothermia and to prevent constriction of tail vessels. Three consecutive measurements of systolic blood pressure/SBP were averaged for each animal at every sequential point of time.

### **3.4. Assessment of Intima-Media Thickness of carotid arteries, *in vivo***

Two-dimensional ultrasound was performed under inhalation anesthesia at the beginning of the study and on the week of sacrifice. Intima-media thickness/IMT of carotid arteries was measured under mild anaesthesia, using a VEVO 770 high-resolution ultrasound imaging system equipped with a 40 MHz transducer.

### **3.5. Isometric force measurement of carotid arteries**

The method was performed in accordance with a standard protocol using common carotid arterial/CCA rings isolated from 4 rats each group. The isometric contractile force was measured by using standard bath procedures in oxygenated physiological Krebs solution. The rings were pre-contracted and equilibrated for 60 minutes until a stable resting tension was acquired. Vasorelaxation is expressed as a percentage reduction of the steady-state tension, obtained with isotonic external 60 mM KCl. Cumulative response curves of carotid rings were obtained in the presence of increasing doses ( $10^{-9}$  to  $10^{-5}$  M) of sodium nitroprusside/SNP, or acetylcholine/ACh. Arterial rings showing relaxation to ACh of more than 30% were considered as endothelium-intact. At the end of the experiments, administration of 60 mM KCl was repeated towards effectively examining the viability of the carotid arteries. Each measurement was carried out on rings prepared from different rats.

### **3.6. Confocal laser scanning fluorescence microscopy**

Left carotid arteries of four rats from each group were fixed immediately following excision in a buffered paraformaldehyde solution/PFA (4%) overnight at 4°C. Five micrometer thick sections were cut and processed for immunolabeling with antibodies recognizing

apoptosis inducing factor/AIF, NF- $\kappa$ B and MAPK phosphatase-1/MKP-1. Sections were counterstained with Hoechst and examined using a confocal laser scan microscope (Olympus Fluoview 1000). Recording for Rhodamine Red<sup>TM</sup>-X was followed by recording for Hoechst.

### **3.7. Histochemical observations**

#### **3.7.1. Carotid arteries**

Paraffin-embedded carotid slices were stained with Masson's trichrome to detect interstitial fibrosis and quantified with the NIH ImageJ analyzer system using the color deconvolution plugin to separate the blue collagen staining and measure its coverage. Measurements were normalized to the tissue-covered area and presented as area percentage (area%). Values of three non-overlapping segments of the tunica media on each preparation were averaged.

#### **3.7.2. Dorsal hippocampus**

Following ketamine/xylazine anesthesia and then thoracotomy, the aortic root was cannulated and the right femoral artery incised to ensure proper effluence. Animals were perfused with physiological saline solution to rinse blood away from the vasculature followed by buffered PFA. Following decapitation, the brain was removed, the hemispheres separated and post-fixed in PFA overnight at 4°C. After embedding in paraffin, coronal sections were taken at the position of bregma approx. (-4.3) – (-3.8) (Paxinos&Watson). Slices were processed for Periodic acid-Schiff/PAS or Cresyl violet staining. Hippocampal pyramidal cell counting was limited between the CA1-CA2 border and the lowest point of CA1-enthorhinal cortex transition on Cresyl violet preparations. TUNEL test was conducted on embedded brain tissue samples in accordance with the manufacturer's protocol. All histological samples were acquired and examined by an investigator in blind fashion.

### **3.8. Immunohistochemistry**

#### **3.8.1. Carotid arteries**

Carotid slices were also processed for NT immunohistochemistry. Binding was visualized with biotinylated-horseradish peroxidase conjugated secondary antibody followed by the avidin-biotin-peroxidase detection system using 3,3'-diaminobenzidine/DAB as chromogen.

#### **3.8.2. Dorsal hippocampus**

Brain sections were processed for immunohistochemistry with antibodies recognizing the following antigens: NT, 4-hydroxynonenal/4-HNE, anti-poly(ADP-ribose)polymer/PAR, 8-oxoguanine/8-OxG and glial fibrillary acidic protein/GFAP. Immunolabeling was visualized by DAB as a chromogen with Universal Vectastain ABC Elite Kit.

### **3.9. Transmission electron microscopy**

Following ketamine/xylazine anesthesia and then thoracotomy, hearts were perfused in retrograde, through the aortic root with ice-cold phosphate buffered saline/PBS to rinse blood away, followed by modified Kranovsky fixative (2% PFA, 2, 5 % glutaraldehyde, 0, 1 M Na-cacodylate buffer, pH 7.4 supplemented with 3 mM CaCl<sub>2</sub>). Next, 1mm thick sections were taken from the free wall of the left ventricle. Dehydrated blocks were submerged in Durcupan resin and then embedded in gelatine capsules containing Durcupan. 1 μm thick semithin and serial ultrathin sections (70 nm) were cut with a Leica ultramicrotome, and mounted either on mesh, or on Collodion-coated single-slot, copper grids. Additional contrast was provided with uranyl acetate and lead citrate solutions. The preparations were examined utilizing a JEOL1200EX-II electron microscope. Areas of inter-fibrillar mitochondria/IFM were measured by freehand polygon selection (n~500/group) in ImageJ software, where length of longitudinal axes and numbers of mitochondrial cristae were also evaluated.

### **3.10. Western blot**

#### **3.10.1. Whole cell preparations**

50 mg of heart samples from the left ventricle wall were homogenized in ice-cold isolation solution, and then samples were centrifuged at 750 G for 12 minutes. Supernatants were harvested in 2× SDS–polyacrylamide gel electrophoresis sample buffer and denatured at 95°C for 5 minutes.

#### **3.10.2. Subcellular fractionation**

Heart tissue was minced in ice-cold isolation solution, and samples were disrupted on ice by Turrax, then processed in a Potter-Elvehjem tissue homogenizer. Centrifugation was carried out for 12 minutes at 750 g. Subsequently, supernatants containing the cytosolic and mitochondrial fractions were aspirated and the precipitate nuclear fraction was discarded. Next, supernatants were centrifuged for 12 minutes at 11,000 g to gain cytosolic fraction in the supernatant and mitochondrial in the precipitate. Subcellular fractions were harvested separately in 2× SDS–polyacrylamide gel electrophoresis sample buffer and denatured at 95°C for 5 minutes.

#### **3.10.3. Electrophoresis and transfer of proteins**

Proteins were separated on 7 or 10% SDS–polyacrylamide gels then transferred to a nitrocellulose membrane. After blocking, membranes were probed overnight at 4 °C with antibodies recognizing the following antigens: dynamin related protein-1/DRP1, optic atrophy protein-1/OPA1, anti-PAR. As a loading control, Glyceraldehyde 3-phosphate dehydrogenase/GAPDH and pyruvate dehydrogenase complex/PDC, were used for whole cell or cytoplasmic fraction and mitochondrial fraction, respectively. Following washing cycles preceding the addition of goat anti-rabbit/mouse horseradish peroxidase-conjugated secondary antibody membranes were incubated at RT for 2 hours. The antibody–antigen complexes were visualized by means of enhanced chemiluminescence. Results were quantified in the NIH ImageJ program. Densities of bands were normalized to the respective loading controls.

### 3.11. Statistical analysis

Normal distribution of group data was checked by the Shapiro-Wilk test. Baseline comparisons between the strains were made by independent samples t-test. Measurements on carotid arteries and the dorsal hippocampus were analyzed by a strain x treatment two-way analysis of variance/ANOVA with 2 levels of each factor, followed by an independent samples t-test in case of factor interactions. On mitochondrial data, one-way ANOVA with Welch correction was conducted followed by Dunnet's *post hoc* test, to reveal the statistical significance of the differences compared to the SHR-C group. Due to the non-normal distribution of data, mitochondrial area and longitudinal axis length measurements were analyzed by the Kruskal-Wallis test followed by *post hoc* pairwise comparisons in SPSS 21.0. All data are presented as mean±S.E.M and  $p < 0.05$  was considered statistically significant.

## 4. Results

### 4.1. Specific Aim I. Evaluation of chronic hypertension-induced vascular remodeling in SHR animals at the level of carotid arteries, in light of long-term pharmacological inhibition of PARP-1.

#### 4.1.1. **Long-term L-2286 administration attenuated the structural and functional remodeling of carotid arteries in hypertensive animals**

Elevation of systolic blood pressure in the SHR strain was significant throughout the study, the applied treatment did not exert any significant effect on this parameter.

At the age of 42 weeks, measurements of IMT in carotid arteries demonstrated profound alterations in SHR animals compared to normotensive controls, by a nearly two-fold increase in wall thickness. Although PARP inhibition attenuated this elevated blood pressure induced process, it did not have any significant effect in normotensive animals regarding this parameter. Quantifying area coverage of collagen bundles on Masson's trichrome stained sections, revealed an extensive accumulation in the middle portion of carotid walls of SHR-C animals at the age of 42 week. The lowered thickening of carotid walls in treated hypertensive rats was accompanied by a substantial decrease in collagen content compared to the control group.

During the pathogenesis of hypertension, a boosted production of  $O_2^-$  in the vasculature leads to vasomotor disturbances by reacting with the potent vasodilator NO, to form ONOO<sup>-</sup>. Visualizing ONOO<sup>-</sup>- modified lipoprotein content of carotid walls by immunohistochemistry revealed an extensive accumulation of nitrated tyrosine residues in SHR-C animals compared to normotensive rats. Long-term L-2286 treatment attenuated level of oxidative stress and NT formation in both strains.

Next, we asked whether the beneficial effect of PARP-1 inhibition against the oxidative damage and structural remodeling of carotid walls will manifest at the functional level. We assessed the vasomotor properties of isolated carotid artery rings against 60 mM KCl pre-contraction, in the presence of increasing doses of ACh or SNP. 32 weeks of L-2286 treatment aided the preservation of endothelium-dependent relaxation capabilities to ACh administration of SHR-L carotid rings. SNP is a NO donor molecule and its effect is dependent on vSMC function. In the presence of the compound, carotid rings isolated from hypertensive rats demonstrated hyper-reactivity, even at lower doses. L-2286 treatment slightly modulated vasomotor responses of SHR-L CCAs for SNP administration, however, the effect was not statistically significant.

#### **4.1.2. Signaling interferences of long-term PARP-1 inhibition in the carotid arteries**

A hallmark of excess PARP-1 activity initiated cell death is the release of AIF from the mitochondrial inter-membrane space and its translocation to the nucleus to initiate large-scale via DNA fragmentation. By confocal microscopy, co-localization of the fluorophore-labeled AIF with the nuclear staining could be observed in a fraction of cellular components only within the control hypertensive group, but not in carotid arteries of L-2286 treated SHRs or normotensive rats.

Hypertension induced phenotypic alterations of various vascular segments are in part, governed by the inflammatory processes related to NF- $\kappa$ B function and an altered cellular physiology of vascular components, as the result of an oxidative and mechanical stress-driven bias in the activity of MAPK members. Immunofluorescent labeling of MKP-1 in carotid arteries revealed an elevated expression in control hypertensive animals relative to WKY groups, which was further increased in L-2286 treated SHRs.

In carotid arteries of control hypertensive rats, activation and nuclear translocation of NF- $\kappa$ B were observed compared to the WKY groups, in which NF- $\kappa$ B could be found predominantly in the extranuclear compartment by confocal microscopy. The above process

was substantially attenuated by long-term L-2286 administration in the carotid arteries of SHR animals.

#### **4.2. Specific Aim II. Observation of chronic hypertension related alterations of the dorsal hippocampus in the SHR strain, focusing on the level of oxidative stress and cell death events.**

##### **4.2.1. Structural alterations of the dorsal hippocampus in the hypertensive animals**

We sought to determine long-term effects of systemic L-2286 administration on TOD in the SHR model, focusing particularly on markers of oxidative stress and consequent damage of the neuronal tissue. For this purpose, the hippocampal area was a suitable model.

On the macroscopic level, brains of the chronic hypertensive rats demonstrated a marked dilatation of cerebral ventriculi. The exerted pressure induced the deformation of the hippocampal structure, as the shortening of its mediolateral axis and deformation of gyrus dentatus with a flattened crest part was apparent (Fig.2). However, long term PARP-1 inhibition had no overt effects on these malformations in treated hypertensive rats, the structure of transverse vessels supplying the hippocampal region was more preserved compared to the irregular lumen shapes observed in the control SHR animals. Lacunar forms of perivascular white matter damage was sporadically present in the SHR-C animals, which alteration was absent in WKY animals and occurred to a much lesser extent in L-2286 treated SHRs.

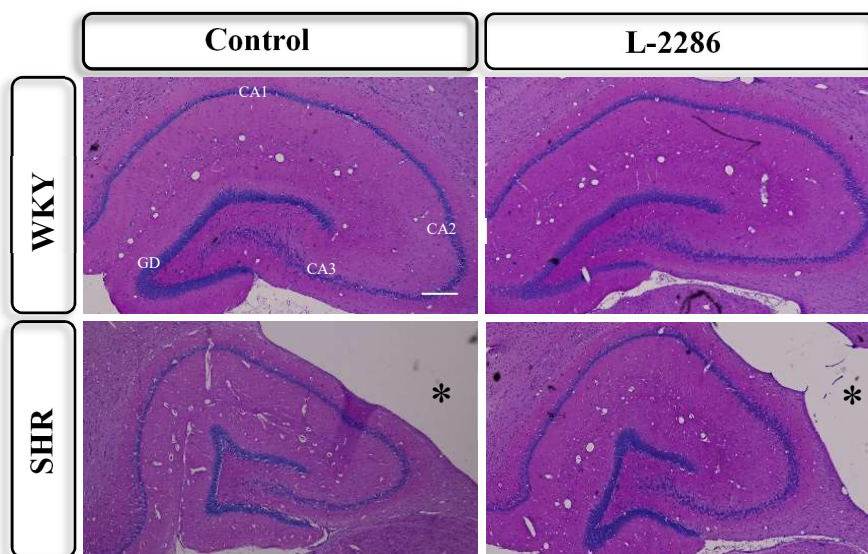


**Figure 2. Chronic hypertension related structural alterations in the rat dorsal hippocampus.** The dorsal hippocampus on PAS stained sections of given groups (scale bar: 200  $\mu$ m). GD, gyrus dentatus; CA1, cornu ammonis 1; CA2, cornu ammonis 2; CA3, cornu ammonis 3; \* marks the lateral cerebral ventriculus.

#### **4.2.2. Systemic L-2286 administration in SHR animals attenuated oxidative damage in the area of dorsal hippocampus**

To assess levels of oxidative damage of lipoproteins and lipids, we labeled brain sections by NT and 4-HNE immunohistochemistry, respectively. During these observations, hypertension related accumulation of nitrated tyrosine residues and the increased peroxidation of lipid membranes were apparent in cellular components and fiber tracts of the hippocampal area of control SHRs. As a sign of attenuated ROS production, long-term L-2286 treatment lowered accumulation of both NT and 4-HNE products in this area of treated hypertensive rats. We also evaluated oxidants induced base-modifications of the DNA in pyramidal cells of the CA1 region by immunohistochemistry to visualize 8-oxoG products (Fig. 8C). In SHR-C animals, a higher portion of 8-oxoG labeled nuclei was observed compared to the normotensive groups in this area. The extent of oxidative DNA damage in pyramidal cells was attenuated by the applied treatment in SHR animals. Taken all together, in chronic hypertensive rats a substantially elevated level of oxidative stress was revealed in the dorsal hippocampal area, as a model for hypertension-related damage of the neuronal tissue. This process and consequent damage of biomolecules were substantially attenuated by long-term pharmacological modulation of PARP-1 activity in SHR animals.

#### **4.2.3. Long-term L-2286 administration attenuated pyramidal cell loss in the CA1 area of treated SHR animals**

Next, we evaluated whether the increased level of oxidative stress and related DNA damage may lead to excess PARP-1 activation in the CA1 region of hypertensive animals. Delineating the results of 8-oxoG observations regarding oxidative damage of DNA, an elevated level of PAR polymer formation was found, with a typical marginal staining of the nuclei in CA1 pyramidal neurons of SHR animals relative to their normotensive counterparts. Long-term PARP-1 inhibition via L-2286 treatment resulted in a lowered intensity of PAR staining in treated animals of both strains. We hypothesized the observed PARP-1 activation may initiate cell death events, therefore quantified pyramidal cell numbers on Cresyl violet stained sections in the CA1 region. The results revealed a marked atrophy of this area by a

significantly lower cell number in SHR animals. Pharmacological modulation of PARP-1 activity led to a more preserved cellular content of the CA1 region in hypertensive rats.

To elucidate “on-going” processes of pyramidal cell loss, we applied the TUNEL-test on brain slices to mark nuclei with a fragmented DNA content. In this observation, the reduced CA1 cell number of hypertensive rats was accompanied by a higher fraction of TUNEL positive nuclei. While 32 weeks of L-2286 administration had no overt effect on cellular content or incidence of cell death events in the CA1 region of WKY animals, treated hypertensive rats demonstrated a more preserved status regarding these parameters.

Astroglial activation in the neuronal tissue indicates a perturbative microenvironment, in which glial cells respond by an increase in their size (hypertrophy) or numbers (hyperplasia) to support functions of neurons or the endothelial cells forming the BBB. We immunolabeled the intermediate-filament GFAP to evaluate the perivascular distribution of this glial subpopulation. No profound difference was found in the number of astrocytes between the strains at the area of the hippocampal fissure, although an alteration in their size as a sign of hypertrophy and a pronounced perivascular immunoreactivity were observed in chronic hypertensive animals. 32 weeks of treatment by L-2286 reduced astroglia numbers in both strains with marginal effect on their reactive hypertrophy in SHR animals. The perivascular presence of reactive astrocytes was attenuated by applied treatment.

### **4.3. Specific Aim III. To elucidate evidence of mitochondrial protection achieved by long-term PARP-1 inhibition in the myocardium.**

#### **4.3.1. Ultrastructural observations on the interfibrillar mitochondria population in the myocardium**

Longitudinal sections were taken to evaluate the *status quo* of interfibrillar mitochondria on electron microscopic preparations in the myocardium of 42 weeks old SHRs, with or without L-2286 treatment. In the SHR-C group, a morphologically more heterogeneous population was observed with partial loss of electron density in the mitochondrial matrices. These mitochondria were loosely packed between the myofilaments demonstrating an intensely disorganized picture relative to the WKY myocardium. Observing the mitochondrial inner membranous structures in normotensive animals we found the cristae to be densely packed, forming regular, wrinkled shapes. In contrast, the reduced number of inner membranes and dilation of cristae spaces and junctions was apparent in control hypertensive rats. The myocardium of L-2286 treated SHR

rats demonstrated an intermediate phenotype with regional heterogeneity, yet a more preserved inner structure, and cristae numbers of interfibrillar mitochondria.

#### 4.3.2. Quantifying the actual state of interfibrillar mitochondrial dynamics

In order to gain insight into the actual equilibrium of fusion-fission processes, we measured the area and the length of the longitudinal axis of interfibrillar mitochondria on electron micrographs (~500 mitochondria/group). The results issued a profound decrease in the mean mitochondrial area of SHR-C group with the shortening of longitudinal axes in comparison to WKY animals, suggesting a more fragmented phenotype in the hypertensive rats. The values of L-2286 treated SHRs differed significantly from the control hypertensive group regarding both mitochondrial area and the lengths of longitudinal axes. Next, we assessed relative frequencies of measured mitochondrial areas in arbitrary intervals of  $0.3 \mu\text{m}^2$  and found a transition towards the lowest interval in the SHR-C myocardium, where nearly half of measured mitochondria had an area lower than  $0.3 \mu\text{m}^2$ . This skewness of area values was attenuated in treated SHR animals and, similar to the normotensive group, the majority of measured mitochondria featured area values above  $0.3 \mu\text{m}^2$ .

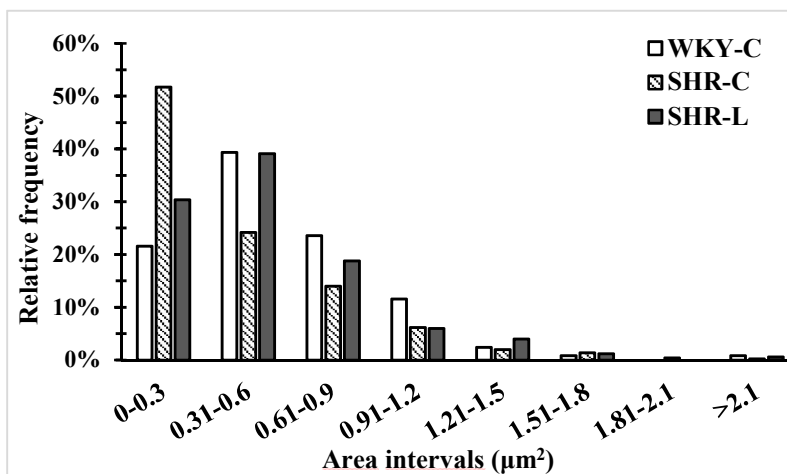


**Figure 3.: Hypertension related fragmentation of interfibrillar mitochondria in the SHR myocardium.** Relative frequencies of measured mitochondrial areas in arbitrary intervals of  $0.3 \mu\text{m}^2$ .

#### 4.3.3. Effects of L-2286 treatment on cellular levels and subcellular distributions of fusion-fission regulators.

We sought to determine levels of OPA1 and the fission mediator DRP1, in the myocardium in whole cell and fractionated Western blot samples, to gain insight at the

molecular level of attenuated fission processes and preserved inner mitochondrial structures in treated hypertensive animals.

First, we assessed the efficacy of L-2286 treatment in whole cell preparations by the extent of auto-PARylation. The highest PAR-polymer formation was observed in control hypertensive animals in comparison to the low signal in the WKY group. L-2286 administration diminished the activity of PARP-1 in treated SHR. In respect to DRP1, we found no overt differences in its cellular levels across the groups although, when observing fractionated samples, a significantly higher portion was observed in mitochondrial fractions of SHR-C animals relative to normotensive controls, as a possible sign of accentuated translocation and anchorage to the outer mitochondrial membrane. Long-term PARP-1 inhibition in hypertensive rats resulted in the retention of a greater portion of DRP1 in the cytosolic fraction relative to SHR-C samples, with a lowered translocation to mitochondria. Cellular levels of OPA1, regulating the integrity and fusion of inner mitochondrial membranes, was significantly reduced in hypertensive animals with only a marginal elevation due to L-2286 treatment, not reaching the level of statistical significance.

## **5. Discussion**

At the age of 42 weeks, our results revealed profound differences in chronic hypertensive animals compared to their normotensive counterparts, regarding structural alterations of carotid arteries and the accumulation of oxidative biomarkers in the observed tissues. Although the applied L-2286 treatment did not exert a significant effect on the elevated blood pressure of SHR animals as the causative factor, it moderated structural and functional remodeling of carotid arteries and, also lowered the level of oxidative damage evaluated in the supplied tissues. Nitrate modification of lipoproteins by accentuated ONOO<sup>-</sup> formation was assessed by immunohistochemistry, at the level of carotid arteries and the dorsal hippocampus. In the latter area of hypertensive rats, our research established enhanced levels of oxidative damage to lipid membranes visualized by 4-HNE staining, and oxidative base-modification of the DNA in CA1 pyramidal neurons accompanied by elevated PAR formation and cell loss. In the myocardium of SHR animals, a more fragmented phenotype of IFM and activation of PARP-1 were demonstrated, as an indirect marker of elevated oxidative stress. These observations demonstrate, how in the SHR strain a hypertension-related enhancement of oxidative stress drives the pathological characteristics of TOD.

Cellular oxidative stress is the result of an insufficient antioxidant capacity in the face of boosted ROS production by various enzyme systems, including the mitochondrial ETC. It in turn confers deleterious effects by the diminished bioavailability of the potent vasodilator NO via ONOO<sup>-</sup> formation, inducing dysregulation of the vascular tone. As a result, endothelial dysfunction of carotid arteries isolated from hypertensive rats was observed by the impaired relaxation capabilities in the presence of ACh. Although the hyper-reactivity of SHR vessels to SNP was not affected by the long-term L-2286 administration in a significant manner, the endothelium-dependent relaxation capability of isolated carotid arteries was more preserved in treated hypertensive animals accompanied by lowered NT accumulation. The inflammatory status of the vasculature during hypertension, indicated by the accentuated nuclear activity of NF-κB in carotid arteries of SHR animals, may further augment the latter process as activation of PARP-1 enhances the expression of pro-inflammatory mediators in the vasculature via NF-κB function furthering ONOO<sup>-</sup> formation via immunological processes and iNOS activity. In this manner, the long-term pharmacologic modulation may have contributed to the lowered nitrate damage and endothelial protection observed in carotid arteries and dorsal hippocampus of L-2286 treated hypertensive animals. A growing body of data demonstrates in which PARP-1 inhibition attenuates the severity of vascular endothelial dysfunction and is even capable of reversing these processes, although the preserved endothelium-dependent vasomotor response of SHR-L animals in our study was not manifested in altered blood pressure. Although applied treatment had no overt effects on the hydrocephalus present in SHR animals, the endothelial protection by L-2286 administration was indicated by the preserved structure of transverse vessels in the hippocampal fissure and lowered perivascular presence of activated astroglia and lacunar white matter damage in treated hypertensive animals. The results above indicate, the protective mechanisms of PARP-1 inhibition in the chronic hypertensive model are not primarily related to altering the mechanical factors to lower vascular stretch or cardiac work demand in the face of elevated blood pressure or even the excess CSF production leading to structural alterations of the dorsal hippocampus, but are most likely based on the attenuation of an aggravated cellular stress responses and tissue inflammation.

Our observations regarding the moderated thickening of carotid artery walls in the treated hypertensive group, despite an arterial pressure comparable to control SHR animals, further delineates the importance of the signaling interference. Activation of various members of MAPK signaling cascade initiating transcriptional programs resulting in proliferation, hypertrophic response and migration of vSMCs, collagen accumulation, initiation of cell death programs and inflammation in the stressed tissues. MKP-1 has low expression in various tissues

during basal conditions, however in stress scenarios, due to a negative feed-back loop, increased MAPK system activation leads to upregulated transcription of the *DUSP1* gene. Recent data demonstrate that during the cellular oxidative stress response, PARP-1 is a negative regulator of MKP-1 expression via its enzymatic activity by modulating the DNA binding of activating transcription factor-4/ATF4. Therefore, the facilitated expression of MKP-1 observed in carotid arteries of L-2286 treated SHRs presumably contributed to the lowered structural remodeling of these vessels by negative regulation of various MAPK members. The above data indicate in which hypertension induced phenotypic changes of the vasculature might be beneficially modulated by the interference of NF- $\kappa$ B and MAPK activation.

In relation to pathological PARP-1 activation, the main source and target of excess ROS production are the mitochondria. In chronic hypertension, vascular alterations related impairment in blood-flow regulation leads to chronic ischemia and metabolic insufficiency of the supplied tissues, which also propagates secondary ROS production via mitochondrial sources. The fragmentation of the IFM reticulum, and the atrophic alteration of hippocampal cortices accompanied by the presence of reactive astrogliosis as an indicator of a metabolically perturbative environment observed in control hypertensive animals delineates these processes. Mitochondrial dysfunction and secondary ROS production are already established in numerous diseases characterized by oxidative stress-related PARP-1 activation. The majority of the responses determining cellular fate converge on the mitochondria, either in a direct or indirect manner. In our study, the observed nuclear translocation of AIF by confocal microscopy in the carotid walls of control hypertensive rats, and also the higher incidence of pyramidal cell nuclei with fragmented DNA in the dorsal hippocampus of these animals indicated “on-going” cell death events governed by oxidant DNA damage, which were profoundly attenuated by long-term pharmacological PARP-1 inhibition in these tissues.

We sought to take qualitative and quantitative assessments on the ultrastructural level regarding the actual state of the cardiac IFM network in the chronic hypertensive rat model. In the electron microscopic preparations, we obtained only a “snap-shot” of these highly dynamic processes defining the actual mitochondrial reticulum structure. However, quantification of individual mitochondrial areas demonstrated a robust alteration in the hypertrophied myocardium of SHR animals, including a shift towards a more fragmented phenotype accompanied by the accentuated translocation of the fission-mediator to the mitochondrial fraction. Our research established the lowered translocation of the fission mediator DRP1 to the mitochondrial fraction, induced by long term pharmacological inhibition of PARP-1. The observation regarding the reduced levels of OPA1 in the hypertrophic myocardium suggests

the presence of mitochondrial damages, consonant with other studies revealing altered levels of fusion mediators in various cardiomyopathies. However, long-term L-2286 treatment resulted in a trend toward higher levels of OPA1 compared to values of SHR-C animals, the induced difference was not statistically significant, and in this way, other mechanisms must have contributed to the more preserved picture of mitochondrial inner membranes in treated animals.

Comprehensively speaking, in the chronic hypertensive rat model, long-term pharmacological PARP-1 inhibition via systemic L-2286 administration, without affecting arterial blood pressure, profoundly moderated hypertensive TOD via an attenuated level of oxidative stress, driving the pathological characteristics of the observed tissues in SHR animals. This effect is primarily based on mitochondrial protection via metabolic stability, attenuated cellular stress responses and additional signaling interferences resulting in a more preserved status of the observed tissues accompanied by a protected cellular content.

## **6. Summary of observations**

- Long-term L-2286 administration moderated the hypertension induced structural remodeling of carotid arteries regarding wall thickening and fibrotic tissue accumulation in SHR animals, without modulating the systolic blood pressure.
- Applied treatment lowered NT accumulation in carotid walls of hypertensive animals and preserved endothelium-dependent relaxation capabilities, as an indicator of attenuated endothelial dysfunction and functional vascular remodeling.
- PARP-1 inhibition interfered the activity of NF- $\kappa$ B and the MAPK system in SHR animals, forming the molecular basis of vascular protection in carotid arteries and in vessels supplying the hippocampal area.
- The elevated levels of oxidative damage of biomolecules in the neuronal tissue of SHR-C animals indicated by NT, 4-HNE and 8-oxoG accumulation were moderated by PARP-1 inhibition, presumably as a result of attenuated secondary ROS production of mitochondrial origin.

- The DNA damage and PARP-1 activation induced cell death events were mitigated in carotid walls of treated SHR animals according to the mitigated nuclear translocation of AIF, also aided to preserve the cellular content of dorsal hippocampus demonstrated by the lowered incidence of TUNEL positive nuclei in the CA1 region.
- The integrity of BBB and cerebral blood supply were improved in treated animals, based on the moderated perivascular presence of activated astroglia population.
- The shift in dynamics of IFM towards a more fragmented phenotype was beneficially affected by long-term L-2286 treatment, accompanied by the lowered mitochondrial translocation of the fission mediator DRP-1.
- The membranous inner structure of SHR cardiac IFM showed a more preserved status related to treatment, however its effect on cellular levels of OPA1 was not statistically significant.

## 7. Publications of the author

(Cumulative impact factor: 30.622)

### 7.1. Relevant publications:

**Krisztian Eros**, Klara Magyar, Laszlo Deres, Arpad Skazel, Adam Riba, Zoltan Vamos, Tamas Kalai, Ferenc Gallyas Jr, Balazs Sumegi, Kalman Toth, Robert Halmosi:

Chronic PARP-1 Inhibition Reduces Carotid Vessel Remodeling and Oxidative Damage of the Dorsal Hippocampus in Spontaneously Hypertensive Rats.

*PLOS ONE* 12:(3) Paper e0174401. 18 p. (2017)

**IF: 2.806**

Klara Magyar, Laszlo Deres, **Krisztian Eros**, Kitti Bruszt, Laszlo Seress, Janos Hamar, Kalman Hideg, Andras Balogh, Ferenc Gallyas Jr., Balazs Sumegi, Kalman Toth, Robert Halmosi:

A Quinazoline-derivative Compound with PARP Inhibitory Effect Suppresses Hypertension-induced Vascular Alterations in Spontaneously Hypertensive Rats.

*Biochim Biophys Acta*. 2014 Jul;1842(7):935-44

**F:4.882**

### 7.2. Additional publications:

Agnes Kemeny, Katalin Cseko, Istvan Szitter, Zoltan Varga, Peter Bencsik, Krisztina Kiss, Robert Halmosi, Laszlo Deres, **Krisztian Eros**, Aniko Perkecz, Laszlo Kereskai, Laszlo Terezia, Tamas Kiss, Peter Ferdinandy, Zsuzsanna Helyes:

Integrative characterization of chronic cigarette smoke-induced cardiopulmonary comorbidities in a mouse model

*ENVIRON POLLUT*. pii: S0269-7491(16)31444-0 (2017)

**IF:5.099**

Eniko Hocsak, Viktor Szabo, Nikoletta Kalman, Csenge Antus, Anna Cseh, Katalin Sumegi, **Krisztian Eros**, Zoltan Hegedus, Ferenc Gallyas Jr, Balazs Sumegi, Boglarka Racz: PARP Inhibition Protects Mitochondria and Reduces ROS Production via PARP-1-ATF4-MKP-1-MAPK Retrograde Pathway.

*FREE RADICAL BIOLOGY AND MEDICINE* 108:770-784 (2017)

**IF: 5.606**

Adam Riba, Laszlo Deres, **Krisztian Eros**, Aliz Szabo, Klara Magyar, Balazs Sumegi, Kalman Toth, Robert Halmosi, Eszter Szabados:

Doxycycline Protects Against ROS-induced Mitochondrial Fragmentation and ISO-Induced Heart Failure

*PLOS ONE* 12:(4) Paper e0175195. 16 p. (2017)

**IF: 2.806**

Robert Halmosi, Laszlo Deres, Roland Gal, **Krisztian Eros**, Balazs Sumegi, Kalman Toth: PARP Inhibition and Postinfarction Myocardial Remodeling.

*INTERNATIONAL JOURNAL OF CARDIOLOGY* 217:(Suppl.) pp. S52-S59. (2016)

IF: 6.189

Laszlo Deres, Eva Bartha, Anita Palfi, **Krisztian Eros**, Adam Riba, Janos Lantos, Tamas Kalai, Kalman Hideg, Balazs Sumegi, Ferenc Gallyas Jr., Kalman Toth, Robert Halmosi:

PARP-inhibitor Treatment Prevents Hypertension Induced Cardiac Remodelling by Favourable Modulation of Heat Shock Proteins, Akt-1/GSK-3 $\beta$  and Several PKC Isoforms. *PLoS One*. 2014 Jul 11;9(7):e102148 (PMID: 25014216) IF:3.234

### 7.3. Published abstracts:

Laszlo Deres, Klara Magyar, Imre Takacs, **Krisztian Eros**, Andras Balogh, Kalman Hideg, Balazs Sumegi, Kalman Toth, Robert Halmosi:

Pharmacological PARP-inhibition Decreases Vascular Fibrosis in Spontaneously Hypertensive Rat Model; *Congress of Hungarian Society of Cardiology 2012. Balatonfüred, Hungary. Cardiologia Hungarica 2012; 42:A21*

Laszlo Deres, Zoltan Vamos, **Krisztian Eros**, Robert Matics, Peter Cseplo, Robert Halmosi, Balazs Sumegi, Kalman Toth, Akos Koller:

Subcellular Aspects of AT1-receptor Mediated Vasomotor Responses in Relation to Age; *Congress of Hungarian Society of Cardiology 2013 Balatonfüred, Hungary. Cardiologia Hungarica 2013; 43:B16*

**Krisztian Eros**, Laszlo Deres, Klara Magyar, Adam Riba, Kalman Hideg, Laszlo Seress, Balazs Sumegi, Kalman Toth, Robert Halmosi:

Effect of PARP-1 Inhibition on the Mitochondrial Fragmentation in an *in vivo* SHR Model. *Congress of Hungarian Society of Cardiology 2013. Balatonfüred, Hungary. Cardiologia Hungarica 2013; 43:B16*

Zoltan Vamos, Laszlo Deres, **Krisztian Eros**, Robert Matics, Ivan Ivic, Andrea Bertalan, Elemer Sipos, Akos Koller, Peter Cseplo:

Age Related Changes of AT1 Receptor Mediated Vasomotor Responses in Isolated Rat Carotid Arteries. *Congress of Hungarian Society of Cardiology 2013. Balatonfüred, Hungary. Cardiologia Hungarica 2013; 43:B32*

**Krisztian Eros**, Laszlo Deres, Klara Magyar, Adam Riba, Kalman Hideg, Laszlo Seress, Balazs Sumegi, Kalman Toth, Robert Halmosi:

Effect of PARP-1 Inhibition on the Mitochondrial Fragmentation in an *in vivos* SHR Model. *VII. International Symposium on Myocardial Cytoprotection 2013 Pecs, Hungary. Cardiologia Hungarica 2013; 43:G12*

Robert Halmosi, Laszlo Deres, **Krisztian Eros**, Klara Magyar, Eva Bartha, Andrea Takacs, Tamas Kalai, Laszlo Seress, Ferenc Gallyas, Balazs Sumegi, Kalman Toth: The Protective Effect of PARP-inhibitors Against Hypertension Induced Myocardial and Vascular Remodeling. *VII. International Symposium on Myocardial Cytoprotection 2013 Pecs, Hungary. Cardiologia Hungarica 2013; 43:G15*

Klara Magyar, Andrea Takacs, Laszlo Deres, **Krisztian Eros**, Laszlo Seress, Zoltan Vamos, Kalman Hideg, Tamas Kalai, Andras Balogh, Akos Koller, Balazs Sumegi, Kalman Toth, Robert Halmosi:

Pharmacological Inhibition of PARP-1 Enzyme Prevents Hypertensive Vascular Remodeling. *VII. International Symposium on Myocardial Cytoprotection 2013 Pecs, Hungary. Cardiologia Hungarica 2013; 43:G20*

**Krisztian Eros**, Eva Bartha, Laszlo Deres, Adam Riba, Tamas Kalai, Kalman Hideg, Balazs Sumegi, Kalman Toth, Robert Halmosi:

Effects of Poly(ADP-ribose)polymerase-1 Inhibition on Myocardial Remodeling in a Chronic Hypertensive Rat Model. *Congress of Hungarian Society of Cardiology 2014. Balatonfüred, Hungary. Cardiologia Hungarica 2014; 44:E51*

Laszlo Deres, **Krisztian Eros**, Noemi Bencze, Laszlo Seress, Balazs Sumegi, Sandor Farkas, Kalman Toth, Robert Halmosi:

The Effects of a Bradykinin B1 Receptor Antagonist on the Development of Hypertensive Organ Damages in SHR Model. *Congress of Hungarian Society of Cardiology 2014. Balatonfüred, Hungary. Cardiologia Hungarica 2014; 44:E25*

Laszlo Deres, **Krisztian Eros**, Noemi Bencze, Laszlo Seress, Balazs Sumegi, Sandor Farkas, Kalman Toth, Robert Halmosi:

The Effects of a Bradykinin B1 Receptor Antagonist on the Development of Hypertensive Organ Damages in SHR Model. *Congress of the European Society of Cardiology 2014. Barcelona, Spain. European Heart Journal (2014) 35 (Abstract Supplement), 664-665.*

Istvan Szitter, Robert Halmosi, Laszlo Deres, **Krisztian Eros**, Krisztina Kiss, Peter Bencsik, Zoltan V. Varga, Peter Ferdinandy, Zsuzsanna Helyes:

Predictive Mouse Model of Chronic Cigarette Smoke-Induced Pulmonary and Cardiac Pathophysiological Alterations. *Joint Meeting of the Federation of European Physiological Societies (FEPS) and the Hungarian Physiological Society 2014. Budapest, Hungary. Acta Physiol (Oxf) 2014 Aug;211 Suppl 697:1-184, Page 106: P5.10.*

Peter Jakus, Nikoletta Kalman, Fruzsina Fonai, Zoltan Hegedus, **Krisztian Eros**, Peter Dombovari, Balazs Sumegi, Balazs Veres:

Cyclophilin D-Dependent mPT Amplifies Inflammatory Response in Septic Shock. *5<sup>th</sup> World Congress on Targeting Mitochondria, 2014. Berlin, Germany. World Mitochondria Society Abstracts Book, Page 177.*

Adam Riba, Laszlo Deres, **Krisztian Eros**, Balazs Sumegi, Kalman Toth, Robert Halmosi, Eszter Szabados:

Protective Effect of Doxycycline Against the Development of Isoproterenol Induced Heart Failure. *Congress of Hungarian Society of Cardiology 2015. Balatonfüred, Hungary. CARDIOLOGIA*

*HUNGARICA 45:(Suppl. D) p. D38. (2015)*

Laszlo Deres, **Krisztian Eros**, Istvan Szitter, Peter Bencsik, Zoltan Varga, Peter Ferdinandy, Kalman Toth, Zsuzsanna Helyes, Robert Halmosi:

The Effects of Chronic Cigarette Smoke Inhalation on Cardiac and Pulmonary Function in Mice. *Congress of Hungarian Society of Cardiology 2015. Balatonfüred, Hungary. CARDIOLOGIA HUNGARICA 45:(Suppl. D) p. D46. (2015)*

**Krisztian Eros**, Arpad Skazel, Klara Magyar, Laszlo Deres, Kalman Hideg, Laszlo Seress, Balazs Sumegi, Kalman Toth, Robert Halmosi:

Systemic PARP-1 Inhibition Attenuates Carotid Vessel Remodelling and Have Protective Effects on Dorsal Hippocampus in Spontaneously Hypertensive Rats. *Congress of Hungarian Society of Cardiology 2016. Balatonfüred, Hungary. CARDIOLOGIA HUNGARICA 46:(Suppl. F) Paper F59.*

Adam Riba, Laszlo Deres, Arpad Skazel, **Krisztian Eros**, Balazs Sumegi, Kalman Toth, Eszter Szabados, Robert Halmosi:

Effects of Resveratrol on Postinfarct Heart Failure in vivo. *Congress of Hungarian Society of Cardiology 2016. Balatonfüred, Hungary. CARDIOLOGIA HUNGARICA 46:(Suppl. F) Paper F43.*

Kalman Toth, Laszlo Deres, Klara Magyar, **Krisztian Eros**, Balazs Sumegi, Robert Halmosi: Myocardial and Vascular Protection by PARP Inhibitors. *3rd European Section Meeting of the International Academy of Cardiovascular Sciences, October 1-4, 2016, Marseille, France.*

*CURRENT RESEARCH: CARDIOLOGY - EXPERIMENTAL CLINICAL 3: p. 90. (2016)*

**Krisztian Eros**, Arpad Skazel, Klara Magyar, Laszlo Deres, Tamas Kalai, Laszlo Seress, Balazs Sumegi, Kalman Toth, Robert Halmosi:

Systemic PARP-1 Inhibition Attenuates Carotid Vessel Remodelling and Have Protective Effects on Dorsal Hippocampus in Spontaneously Hypertensive Rats. *3rd European Section Meeting of the International Academy of Cardiovascular Sciences, October 1-4, 2016, Marseille, France.*

*CURRENT RESEARCH: CARDIOLOGY - EXPERIMENTAL CLINICAL 3: p. 108. (2016)*

## **8. Acknowledgement**

I wish to express my gratefulness to my Program Leader, Professor Kálmán Tóth, and to my Project Leader, Dr. Halmosi Róbert for guiding my studies throughout the field of cardiovascular sciences and providing the possibility of the current work. I'm genuinely appreciative to Professor Balázs Sümegi for mentoring my studies and work in the recent years and for widening my view on systemic biology.

I'm thankful to all my present and former colleagues, especially for Dr. Klára Magyar and for Dr. László Deres, for their contributions and helping hands in the present research. Notably, my sincerest appreciation to Professor László Seress, for his immense field support in respect to hippocampal observations. Additionally, I wish to acknowledge Mrs. Tímea Dózsa and Mr. József Nyiradi, for extending their expertise in support of this body of research.

I want to offer my thanks to Dr. Ildikó Bock-Marquette and Mr. Jon E. Marquette for their encouraging words and mentality throughout these times.

I express my warmest appreciation to my family and close friends for their immense patience and support during the preparation of this work.